

SCIENTIFIC REPORTS



OPEN

Odorant receptors of *Drosophila* are sensitive to the molecular volume of odorants

Majid Saberi & Hamed Seyed-allaei

Received: 02 October 2015

Accepted: 08 April 2016

Published: 26 April 2016

Which properties of a molecule define its odor? This is a basic yet unanswered question regarding the olfactory system. The olfactory system of *Drosophila* has a repertoire of approximately 60 odorant receptors. Molecules bind to odorant receptors with different affinities and activate them with different efficacies, thus providing a combinatorial code that identifies odorants. We hypothesized that the binding affinity of an odorant-receptor pair is affected by their relative sizes. The maximum affinity can be attained when the molecular volume of an odorant matches the volume of the binding pocket. The affinity drops to zero when the sizes are too different, thus obscuring the effects of other molecular properties. We developed a mathematical formulation of this hypothesis and verified it using *Drosophila* data. We also predicted the volume and structural flexibility of the binding site of each odorant receptor; these features significantly differ between odorant receptors. The differences in the volumes and structural flexibilities of different odorant receptor binding sites may explain the difference in the scents of similar molecules with different sizes.

We know which properties of visible light are measured by our eyes, and we also know how our eyes process light. This knowledge has assisted in the production of cameras and displays. Unfortunately, we do not have the same knowledge regarding olfaction. We do not know the relationship between the molecular properties of a stimulus and the sensory response (i.e., the quality of a smell).

Olfactory receptor neurons (ORNs) are at the front end of the olfactory system. Each ORN expresses only one type of odorant receptor (OR). ORNs of the same type converge into the same glomerulus of the antennal lobe in insects (or the olfactory bulb in humans)^{1–9}.

The olfactory system uses a combinatorial code. Unlike many other receptors that are activated by only one specific ligand, such as a neurotransmitter or a hormone, an OR can be triggered by many odorant molecules. Furthermore, an odorant molecule can interact with different types of OR¹⁰. The combinatorial code enables humans to discriminate many odors¹¹ by using a repertoire of only approximately 350 ORs. However, it is not yet clear which properties of a molecule contribute to its smell. This question is a topic of ongoing research, and many theories have been proposed^{12–26}.

Odorant receptors are transmembrane proteins, and in vertebrates, they are metabotropic receptors that belong to the G-protein coupled receptor (GPCR) family^{27,28}. In insects, the signaling methods of ORs are a topic of debate. Insect ORs are thought to be ionotropic receptors but may also use metabotropic signaling^{29–33}. The topology of ORs in insects is different from that in vertebrates^{34,35}, and most insect ORs function in the presence of another common receptor known as Orco³⁶.

Many similarities exist between the olfactory system of insects and that of vertebrates^{37,38}. Regardless of the signal transduction pathway utilized, all ORs have the same function: they have a binding pocket (also known as a binding cavity or a binding site), where odorants (also known as ligands) bind. Binding to an odorant activates an OR, and the activated OR changes the potential of the cell either directly (ionotropic) or indirectly (metabotropic); therefore, knowledge regarding the olfactory system of *Drosophila* could potentially help us to decode human olfaction.

The amplitude of the change in the membrane potential of an ORN depends on the number of activated ORs and the duration of their activation, which are both determined by various physicochemical properties of the odorant and the OR^{12,14,18,39,40}. One important factor is the size of the ligand relative to the OR binding pocket. Another factor is the flexibility of the binding pocket. Proteins are not rigid bodies and can change shape

School of Cognitive Sciences, Institute for Research in Fundamental Sciences (IPM), Tehran, Iran. Correspondence and requests for materials should be addressed to H.S.-a. (email: hamed@ipm.ir)

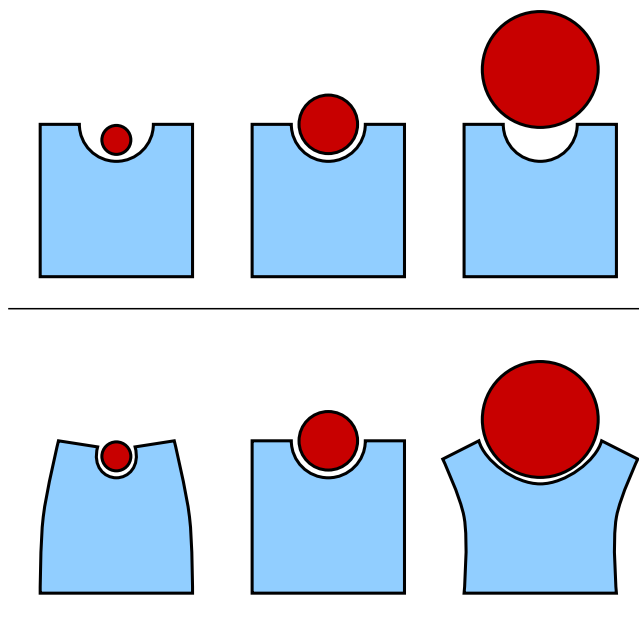


Figure 1. This figure shows different scenarios that may occur when an odorant molecule (ligand) binds to an odorant receptor according to the coarse-grained model. The red disks represent the odorant molecule, and the blue shapes represent the odorant receptor (OR) and binding pocket. The top schematic shows a mismatch because of the small molecular volume on the left, a perfect match in the center and a mismatch because of a large molecular volume on the right. The bottom schematic shows how the flexibility of an OR may compensate for molecular volume mismatches.

depending on the amino acids involved^{41–43}. The size and flexibility of binding pockets have been used in computational drug design to predict the binding pocket of a given ligand⁴⁴.

Herein, we focused on the volume and flexibility of the binding pocket. The molecular volume of a ligand should match the dimensions of the OR binding pocket. Subsequently, the ligand can fit into the binding pocket of the OR and trigger signal transduction. Mismatches in volume decrease the neural response; however, flexibility of the binding pocket can compensate for volume mismatches (Fig. 1).

We can determine the volume and flexibility of a binding pocket if we know its three-dimensional structure. However, the structures or ORs are unknown because it is difficult to determine the structure of integral membrane proteins^{45,46}. To investigate OR protein structure, various research methods have been used, including molecular dynamics (MD) simulations, mutagenesis studies, heterologous expression studies, and homology modeling^{47–55}.

In the current study, we develop a mathematical framework that utilizes available experimental data, and we apply this developed mathematical framework to investigate the relationship between the molecular volume of odorants and the ORN response. Our results suggest that although molecular volume is a considerable factor, it is not the only factor that determines the neural response of ORNs. We predict the *in vivo* volumes and flexibilities of OR binding pockets (supplemental file volume-profiles.csv) by applying our mathematical method to neural data from the Database of Odorant Receptors (DoOR)⁵⁶, which is a well-structured database that includes the neural responses of most *Drosophila* ORs to many odorants⁵⁶. This database aggregates data from many sources^{17,19,57–69}.

We suggest that a functional relationship exists between molecular volume and the neural response. We also provide a methodology to estimate the *molecular receptive range* or *tuning function* of ORs. Finally, we predict the structural properties (i.e., volumes and flexibilities) of OR binding pockets. Our results may aid in the selection of odorants for future experimental studies (supplemental file proposed-odorants.csv) and may contribute to the study of olfactory coding by unmasking the effects of other possible factors.

Material and Methods

We used the neural data of the DoOR 1.0⁵⁶ database for our calculations, and we reserved the additional data in the DoOR 2.0^{18,70–75} database to use as a test set. We calculated the molecular volume (supplemental file odorants.csv) using the computational chemistry software VEGA ZZ⁷⁶. We used GNU R statistical computing software to analyze the data⁷⁷.

The DoOR database includes an $N \times M$ matrix. Its elements, r_{nm} , are the response of ORN n to odorant m . This matrix is normalized to have values between 0 and 1, so $0 \leq r_{nm} \leq 1$, where 1 is the strongest response. This matrix has many *Not Available* (NA) values, and different ORNs are excited by different sets of odorants. We accounted for this feature by removing NA values from the summations and calculating $\sum_{m:r_{nm} \neq \text{NA}}$; however, for brevity, we used the usual notation \sum_m .

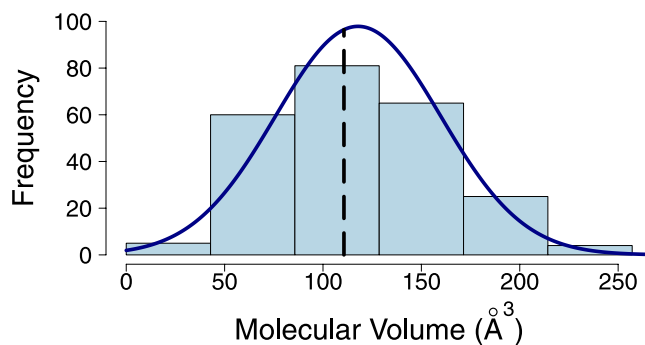


Figure 2. The graph shows the density function of molecular volumes, $g(v)$, for all molecules in the DoOR database. The solid line is a Gaussian fit (Eq. 5), and the dashed line shows the median, which is slightly different from the mean.

The response r_{nm} may depend on the molecular volume of the odorant, v_m , and other physicochemical properties of the molecule m ; therefore, we separated the response r_{nm} into two terms:

$$r_{nm} = f_n(v_m)\psi_{nm}. \quad (1)$$

The first term, $f_n(v_m)$, depends only on the molecular volume of the odorant. The second term, the volume-independent term ψ_{nm} , includes every other influential property of the odorant molecule, with the exception of molecular volume or any other property that correlates with molecular volume (e.g., molecular weight). Of the molecular parameters that correlate with molecular volume, we used molecular volume because it fits the acceptable picture of protein-ligand interaction (Fig. 1). Using molecular weight would have implied receptors use some type of mass spectroscopy analysis. We tested a few other important parameters, including polarity, functional group, and polar surface area; however, none of the parameters were as dominant as molecular volume. Therefore, we primarily focused on molecular volume ($f_n(v)$) and may consider other parameters (ψ_{nm}) in future studies.

Each of the two terms was characteristic of the OR and varied for each OR. In fact, the first term, $f_n(v)$, can be considered to be the tuning curve of an ORN n with respect to the molecular volume. We approximate this term with a Gaussian function,

$$f_n(v) = e^{-\frac{(v-v_n)^2}{2\sigma_n^2}}, \quad (2)$$

where v_n is the preferred molecular volume of the OR n , and σ_n represents the flexibility of the OR binding pocket. We used a Gaussian function for the tuning curve for the following reasons: (a) it is among the simplest forms that can describe a preferred volume and flexibility, and (b) the mathematics was easy to follow and the final solution was simple.

In this work, we wanted to estimate v_n and σ_n . Thus, we first calculated the response-weighted average of the molecular volumes, $\frac{\sum_m v_m r_{nm}}{\sum_m r_{nm}}$, and then we used (1):

$$\frac{\sum_m v_m r_{nm}}{\sum_m r_{nm}} = \frac{\sum_m v_m f_n(v_m)\psi_{nm}}{\sum_m f_n(v_m)\psi_{nm}}. \quad (3)$$

We approximated \sum with \int , which is common in statistical physics:

$$\sum_m \dots f_n(v_m)\psi_{nm} \approx \langle \psi_{nm} \rangle_m \int_0^\infty \dots f_n(v)g(v)dv. \quad (4)$$

In this equation, $\langle \psi_{nm} \rangle_m$ denotes the average of ψ_{nm} over all m : $r_{nm} \neq \text{NA}$. We moved $\langle \psi_{nm} \rangle_m$ out of the integral because it is independent of v . Here, $g(v)$ is the density of states, and $g(v)dv$ indicates how many molecules have a molecular volume in the range of v and $v + dv$. This function was approximated by a Gaussian function (Fig. 2),

$$g(v) = e^{-\frac{(v-v_g)^2}{2\sigma_g^2}}. \quad (5)$$

Ideally, $g(v)$ must not depend on the OR n because it is a property of the ensemble of odorant molecules and not a property of the OR. We also had many missing values ($r_{nm} = \text{NA}$) that did not overlap, and we had to calculate $g(v)$ for each ORN separately; therefore, v_{g_n} and σ_{g_n} are the average and standard deviation, respectively, of the molecular volume while $r_{nm} \neq \text{NA}$. We rewrote equation (3) using equation (4):

$$\frac{\sum_m v_m r_{nm}}{\sum_m r_{nm}} \approx \frac{\int v f_n(v) g_n(v) dv}{\int f_n(v) g_n(v) dv}. \quad (6)$$

To obtain a simpler form, we replaced the product of $f_n(v)$ and $g_n(v)$ in the above equation with $h_n(v) = f_n(v)g_n(v)$.

$$\frac{\sum_m v_m r_{nm}}{\sum_m r_{nm}} \approx \frac{\int v h_n(v) dv}{\int h_n(v) dv}. \quad (7)$$

The function $h_n(v)$ is a Gaussian function because it is the product of two Gaussian functions,

$$h_n(v) = e^{-\frac{(v-\mu_{h_n})^2}{2\sigma_{h_n}^2}}. \quad (8)$$

Thus, the right side of equation 7 was nothing but μ_{h_n} , and in a similar manner, we calculated σ_{h_n} from the neural data.

$$\mu_{h_n} \approx \frac{\sum_m v_m r_{nm}}{\sum_m r_{nm}} \quad (9)$$

$$\sigma_{h_n}^2 \approx \frac{\sum_m v_m^2 r_{nm}}{\sum_m r_{nm}} - \mu_{h_n}^2 \quad (10)$$

We know the mean, v_{g_n} , and standard deviation, σ_{g_n} , of $g_n(v)$ from the molecular volumes of the ensemble of odorants. We calculated the mean μ_{h_n} and standard deviation σ_{h_n} of $h_n(v)$ from the neural data. Using these values, we calculated the mean v_n and the standard deviation σ_n of $f_n(v)$. First, we calculated σ_n using

$$\frac{1}{\sigma_n^2} = \frac{1}{\sigma_{h_n}^2} - \frac{1}{\sigma_{g_n}^2}, \quad (11)$$

and then we calculated v_n :

$$\frac{v_n}{\sigma_n^2} = \frac{\mu_{h_n}}{\sigma_{h_n}^2} - \frac{v_{g_n}}{\sigma_{g_n}^2}. \quad (12)$$

The calculated v_n and σ_n are provided in the supplemental file volume-profiles.csv. The resulting $f_n(v)$ are plotted over the actual data for the 28 ORs (Fig. 3) in which the p-values were < 0.05 .

We calculated p-values using permutation tests and shuffled the data 10^5 times. We shuffled the association between odorants and the responses of a given OR and then checked the null and alternative hypotheses. The alternative hypothesis was that “the response of the ORN depends on the molecular volume of the odorant”, which requires a finite value for σ_n . The null hypothesis was that “the response of the ORN is independent of the molecular volume of the odorant”, which requires $\sigma_n \rightarrow \infty$. Therefore, the p-value is the probability of having $\sigma_n' \leq \sigma_n$, where σ_n is calculated from the original data, but σ_n' is calculated using the permuted version.

We tested the hypotheses on ~60 ORs simultaneously (only 44 were present in the DoOR 1.0 database). Using a simple threshold of 0.05 for the p-value of each OR would have resulted in many false positives. To address the issue of a multiple-comparison problem, we used the Bonferroni correction (by multiplying the p-values by 60). The problem with the Bonferroni correction is that it may increase the number of false negatives. This problem can be addressed by using another method called the false discovery rate (FDR) that keeps the rate of false positives below a threshold^{78,79}. We used the Bonferroni and FDR methods as well as no correction. We used the function *p.adjust* of GNU R to calculate the corrected p-values. The results were labeled accordingly in Figs 3 and 4.

We also wanted to show the diversity of volumes and flexibilities of binding pockets among ORs. To estimate the p-values, we used any pair of ORs that were sensitive to molecular volume (28 ORs), calculated their difference, used a permutation test (6×10^4 shuffles) and measured the probability of obtaining different results (Fig. 5).

Results and Discussions

The relationship between molecular volume and the ORN response was evident (Figs 3–5). The function $f_n(v)$ was considered to be the tuning curve of OR n in response to molecular volume (Fig. 3). Each OR had a preferred molecular volume v_n and showed some flexibility σ_n . The calculated $f_n(v)$ values are shown in Fig. 3. This figure includes 28 ORs that showed a significant dependence on odorant molecular volume in their response (p-value < 0.05).

The flexibility of a receptor may affect the broadness of its tuning curve (flexible receptors may bind to more odorants), but we did not see any significant relationship when using three definitions of broadness: depth of selectivity, breadth of selectivity and kurtosis^{70,80,81}.

The results of 28 ORs indicated that 11 ORs were significant according to the Bonferroni correction (ORs with black names), 26 of them were significant according to FDR correction (ORs with gray names), and the remaining

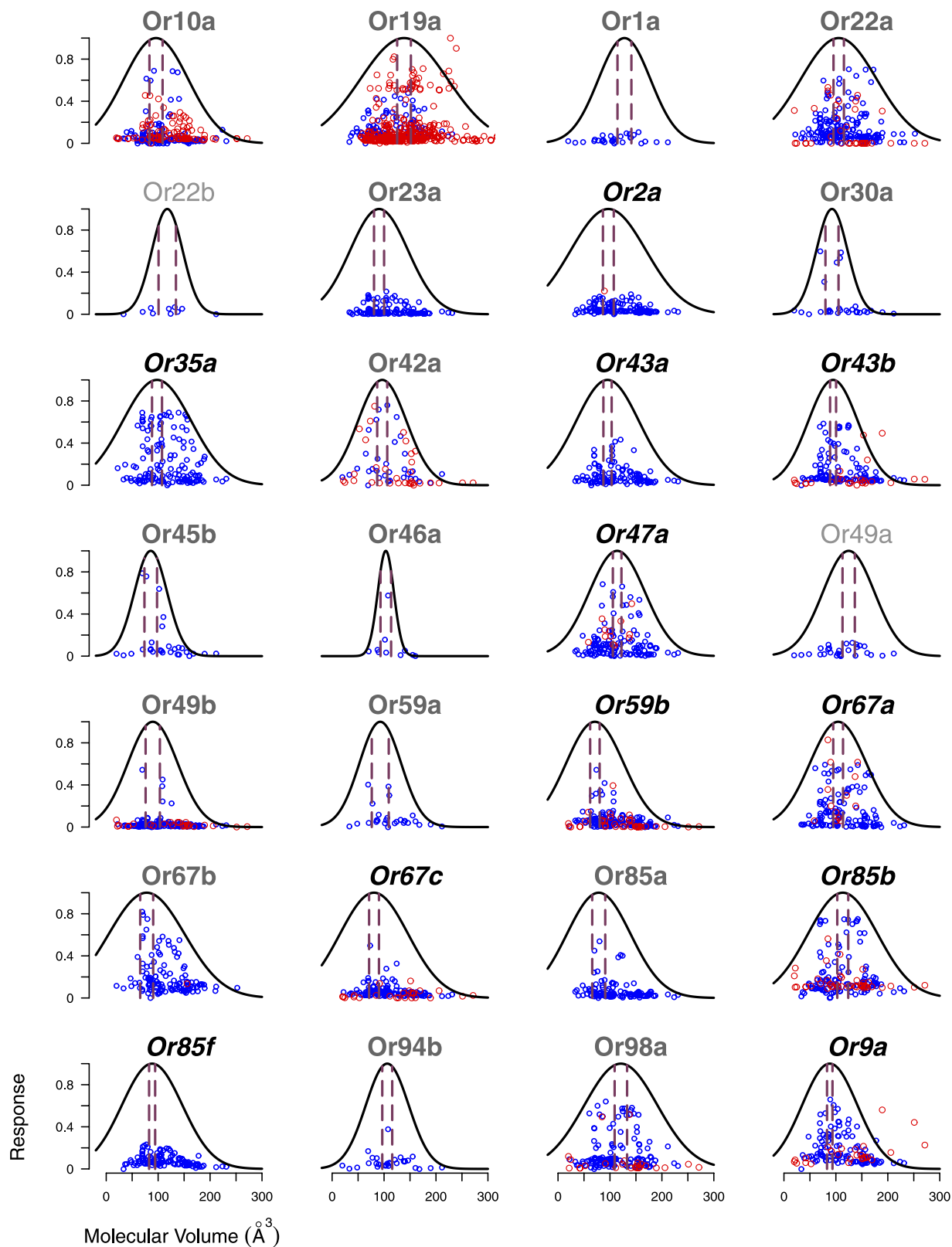


Figure 3. The response of ORs versus the molecular volume of odorants (circles). The fitted functions $f_n(v)$ from Eq. 1 (solid lines) and the error bars of the mean of $f_n(v)$ (red vertical lines) for 28 ORs showed that their responses were significantly dependent (p -value < 0.05) on molecular volume. Except 2 (ORs name in light gray), 26 were significant according to the FDR correction (ORs named in gray), and 11 were significant according to the Bonferroni correction (ORs with names in black). The function $f_n(v)$ was calculated based on data from the DoOR 1.0 database (blue circles). The red circles are additional data from the DoOR 2.0 database.

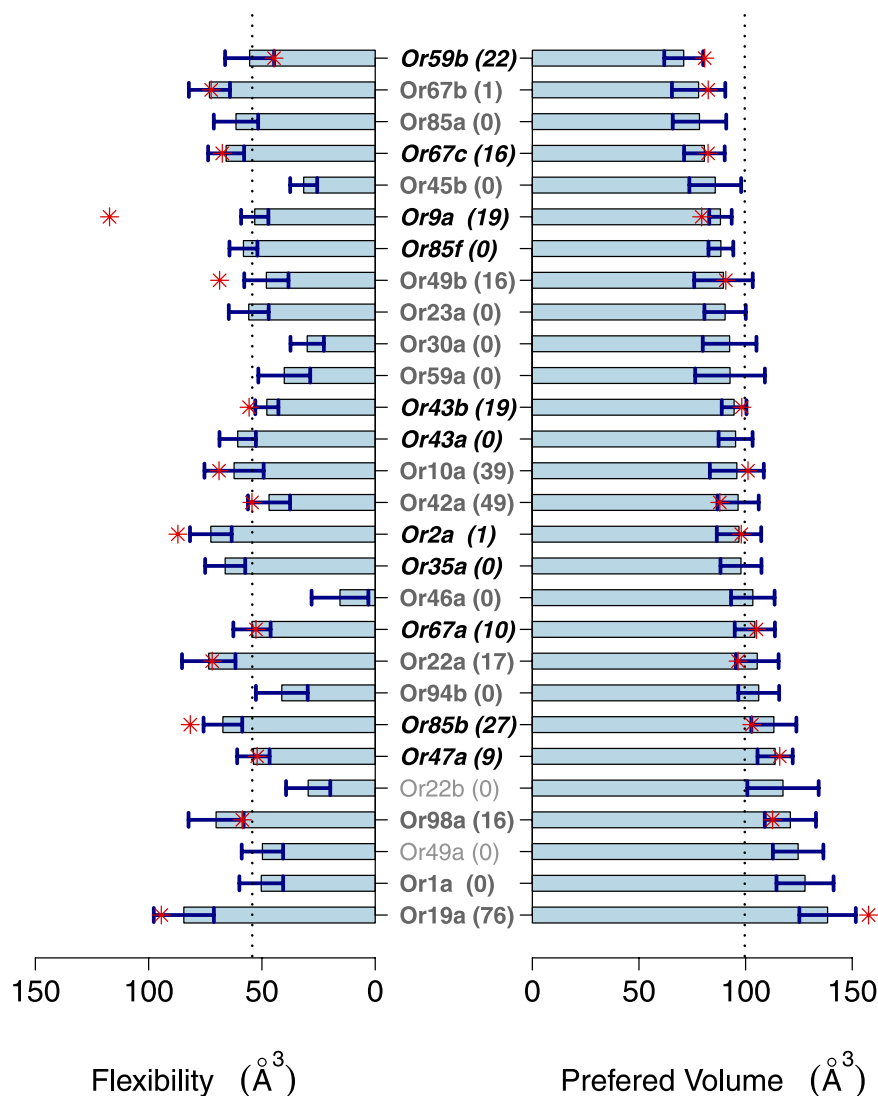


Figure 4. The preferred volumes v_n (right) and flexibilities σ_n (left) of 28 ORs. The error bars were calculated using the Jack-Knife method. Some ORs, including Or59b, Or67a and Or85a, preferred smaller molecules, but some ORs, including Or19a, Or1a and Or49a, preferred larger molecules. Some ORs, such as Or46a, Or22b and Or30a, were volume selective, but other ORs, including Or19a, Or67b and Or22a, responded to a broader range of molecular volumes. Asterisks indicate the updated results using the DoOR 2.0 database, and the numbers in parentheses show the percentage of DoOR 2.0 results relative to the total amount of data for each receptor.

receptors (2 ORs with light gray names) only satisfied the criteria of a p-value < 0.05 without any corrections. After applying the FDR correction, more than half of the available ORs in the DoOR 1.0 database (26/44) showed significant sensitivities toward molecular volume. The remaining receptors may be sensitive to molecular volume as well; however, the current evidence is not sufficient, and more experiments are necessary.

One interesting case in this regard was Or82a, which did not fit our hypothesis. Or82a binds to geranyl acetate much better than to any other molecule. When we removed geranyl acetate from the data, suddenly Or82a fit perfectly to our model with a Bonferroni-corrected p-value of 0.03 (Fig. 6). The underlying interaction between geranyl acetate and Or82a is therefore a special case that requires more investigation.

The parameters of $f_n(v)$, v_n and σ_n are shown in Fig. 4. Figure 4 demonstrates that the molecular volume preferences of ORs were different (right), and the flexibilities of the ORs were also different (left). To support these claims, we estimated the p-values of having different volume preferences and flexibilities for each pair of 28 ORs (Fig. 5). The comparison of the volume preferences of all 378 possible pairs indicated that 133 had a p-value less than 0.05. This number was reduced to 89 after using the FDR correction and further reduced to 32 after using the Bonferroni correction. The corresponding number of pairs with a p-value less than 0.05 was 168, 134 and 77, respectively, for the flexibility comparisons. The union of these two sets confirmed that 226 (p-value < 0.05), 171 (FDR corrected), and 91 (Bonferroni corrected) pairs of ORs showed distinct differences in their binding-pocket characteristics.

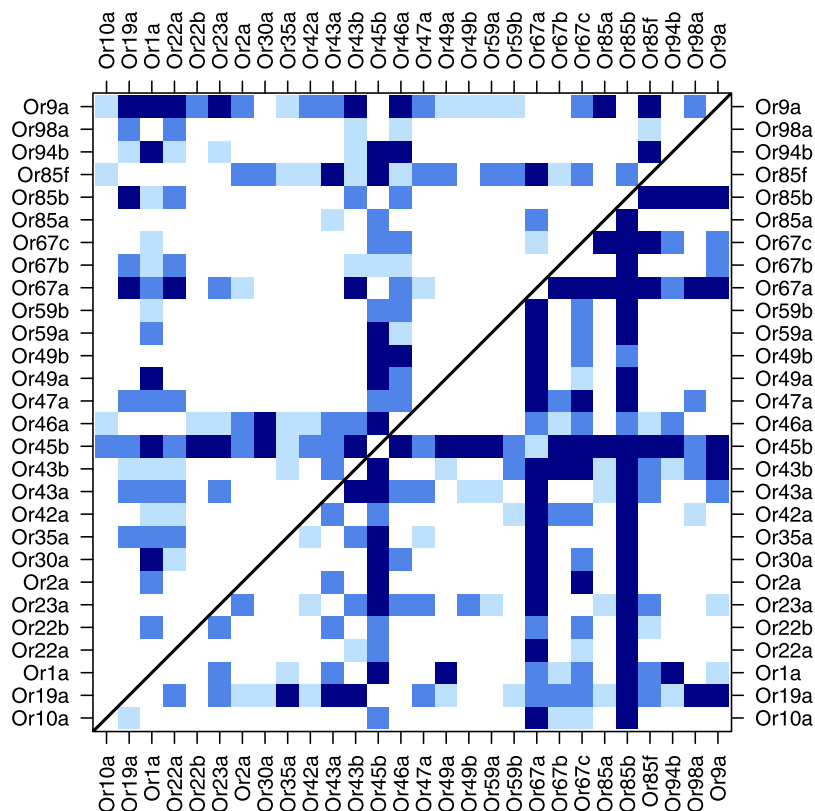


Figure 5. Pairs of ORs that differed significantly in their binding-pocket volumes (upper triangle) and flexibilities (lower triangle). All blue shades indicate a p-value less than 0.05. The two darker shades indicate FDR-corrected p-values less than 0.05, and the darkest shade has a Bonferroni-corrected p-value less than 0.05.

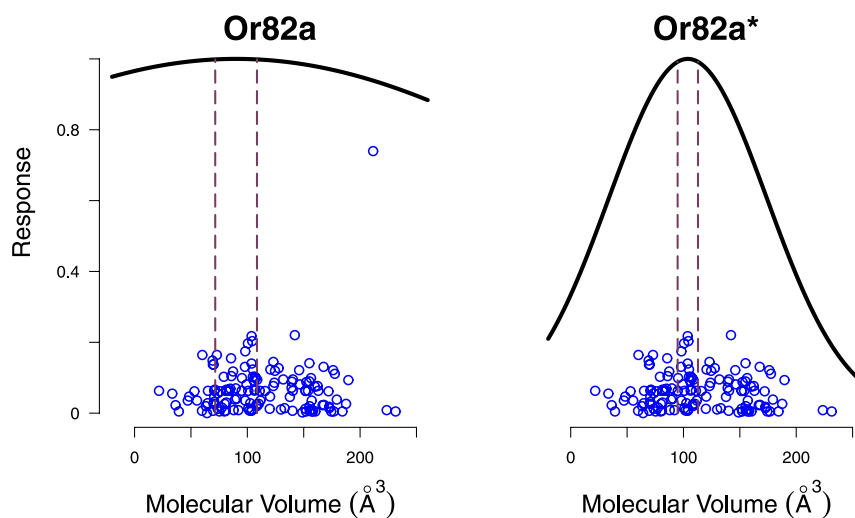


Figure 6. The response of Or82a to odorants. Geranyl acetate (the outlier) did not confirm our theory and had a p-value of 0.55 (left); however, when geranyl acetate was removed from the data, Or82a confirmed our model with a Bonferroni-corrected p-value of 0.03 (right).

The diversity of ORs is important in perceiving the quality of smells. In a hypothetical experiment, assume that all odorant molecule characteristics are the same with the exception of molecular volume. If all ORs have the same preferred volume and flexibility, any change in the molecular volume will change only the intensity of smell and not its quality. Here, we showed that ORs have different preferred volumes and flexibilities. Therefore, any change in the molecular volume of an odorant results in a different combinatorial encoding, which affects the quality and intensity of the perceived smell. This conclusion is in agreement with the work of M. Zarzo that suggested that larger molecules smell better⁸² and might account for differences between the scents of methanol,

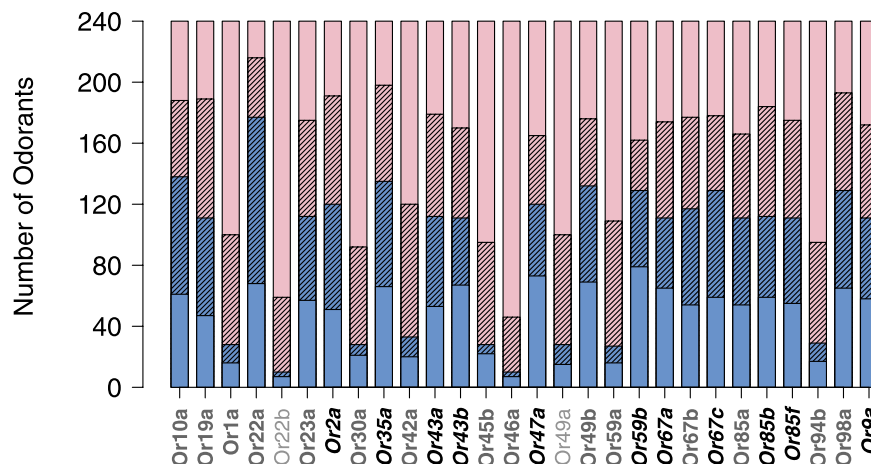


Figure 7. Venn diagram of the DoOR 1.0 database and our suggested important odorants for each OR. The database includes 240 molecules. Some of the 240 molecules have been used to study an OR (blue areas); however, data for the rest of the molecules are not available for some of the ORs (pink). The hatched areas represent odorants with molecular volumes that are close to the preferred volume of each OR ($v_n \pm \frac{\sigma}{2}$). We already know the neural responses of the hatched blue areas, but the hatched pink odorant areas can be the target of future experiments. We predict that the remaining odorants will only yield no response.

ethanol, propanol and butanol. Methanol smells pungent, ethanol smells pleasant and wine-like, and propanol and butanol smell like ethanol; however, butanol has a slight banana-like aroma. We argue that molecular volume affects combinatorial encoding and that combinatorial encoding determines odorant quality.

Herein, we showed that the responses of ORNs are related to odorant molecular volume. However, it is not clear what other features of molecules are measured by ORs. Many studies have attempted to connect the physicochemical properties of molecules to the evoked neural response and/or the perceived smells; however, the nonlinear volume dependence (Eq. 1 and Eq. 2) may mask important correlations between molecules and neural responses. When $f_n(v)$ is close to zero, the value of ψ_{nm} does not matter.

We predicted that odorants with a molecular volume in the tail regions of $f_n(v)$ remain undetected, regardless of any of their other physicochemical properties. This prediction can be confirmed in future experiments.

When studying the ψ_{nm} of an OR, it is better to have many data points, and it is better for the data points to be close to the preferred volume of the OR; however, the current data do not meet these conditions. For many ORs, most data points are in the tail regions of $f_n(v)$, with values close to zero. We have included the best selection of odorants for each of the 28 studied ORs (see Venn diagram in Fig. 7 and supplemental file proposed-odorants.csv); this information can be used to save time and expenses during future experiments.

We have also predicted some *in vivo* structural aspects of OR binding pockets: the preferred volume of each OR results from the volume of the binding pocket, and the flexibility of an OR results from the rigidity or flexibility of the binding pocket. These data provide additional constraints on the 3D structure of ORs, which may aid in the prediction and calculation of the 3D structure of these proteins.

The methods of the current study can also be combined with mutagenesis. When an OR gene is mutated, the response to a selection of molecules can be subsequently measured, and finally, the preferred volume and flexibility can be calculated. In this way, we could potentially understand which amino acids affect the function of the OR and contribute to both the volume and flexibility of the binding pocket.

In this manuscript, we have excluded many factors because the nature of the problem is inherently complex; it would not be feasible to study this problem with all possible factors. Many factors affect the concentration of odorant molecules at ORs, including the molecular mass, the method of mixing odorants and air, the vapor pressure, the solubility of odorants in water, the sensillum lymph and odorant-binding proteins (e.g., LUSH)^{83,84}. It is difficult to control for all of the aforementioned factors in the current experimental paradigm, and the model would be very complex with many sets of parameters. For example, if we introduce an odorant into air, there will be a mixture of air, vapor and mist. Then, the mixture reaches the sensilla, mixes with sensillum lymph fluid, may bind to odorant-binding proteins and finally reaches ORs. Two important parameters in this process are vapor pressure and water solubility. Vapor pressure limits the vapor concentration of a liquid. Water solubility limits the amount of odorant that can dissolve in water. Both factors are nonlinear at high concentrations; therefore, we can neglect the effect of vapor pressure and water solubility. However, if we are close to the critical concentrations, vapor pressure and water solubility are very important.

We expect these factors to have minimal effects on smaller molecules because they evaporate easily, readily dissolve in water and might not need the help of odorant-binding proteins. Therefore, we have greater confidence about the lack of response to small molecules than we do about the lack of response to larger molecules. Using an experimental paradigm similar to a luciferase assay⁸⁵ may provide valuable complementary information to our simple model. When using a luciferase assay, the concentrations are accurate, but the experiment is *in vitro*.

Conclusion

We showed that molecular volume is an important factor, but it is not the only factor that determines the response of ORNs.

We hypothesized that the ORN response results from OR binding-pocket volume and flexibility. We predicted the actual *in vivo* volumes and flexibilities of OR binding pockets. The results are provided in supplemental file volume-profiles.csv, and they can be verified when the 3D structures are resolved and/or when more experimental results are available.

Now that we understand the extent to which molecular volume contributes to the ORN response, it is possible to study the effects of other parameters.

We approximated a molecule as a rigid isotropic sphere of a given volume, but our model does not consider the shape^{13,14,40}, vibrational mode^{12,16,24}, chirality⁸⁶ or many other potentially interesting properties of a molecule. Our methods and results actually provide a starting point that may lead to the study of other factors.

An improvement to this model would be to include the anisotropy of the molecules by modeling them as ellipsoids. This modeling will capture more aspects of the molecular shape and may aid in the inclusion of conformational isomers.

Approximating $f_n(v)$ and $g(v)$ with a Gaussian function makes the mathematical formulation simple and readable. However, a semi-infinite function may be a better choice for molecular volumes, which cannot have negative values.

Although this work utilized data from *Drosophila*, we expect that the general principles and methodologies of this work will also apply to vertebrates. We are working to apply the same method to human odorant receptor data⁸⁵.

References

1. M. Root, C., Semmelhack, J. L., Wong, A. M., Flores, J. & Wang, J. W. Propagation of olfactory information in drosophila. *Proc. Natl. Acad. Sci.* **104**, 11826–11831, doi: 10.1073/pnas.0704523104 (2007).
2. Carey, A. F. & Carlson, J. R. Insect olfaction from model systems to disease control. *Proc. Natl. Acad. Sci.* **108**, 12987–12995, doi: 10.1073/pnas.1103472108 (2011).
3. Vosshall, L. B., Wong, A. M. & Axel, R. An Olfactory Sensory Map in the Fly Brain. *Cell* **102**, 147–159, doi: 10.1016/S0092-8674(00)00021-0 (2000).
4. Couto, A., Alenius, M. & Dickson, B. J. Molecular, anatomical, and functional organization of the *Drosophila* olfactory system. *Curr. Biol.* **15**, 1535–1547, doi: 10.1016/j.cub.2005.07.034 (2005).
5. Fishilevich, E. & Vosshall, L. B. Genetic and functional subdivision of the *drosophila* antennal lobe. *Curr. Biol.* **15**, 1548–1553, doi: 10.1016/j.cub.2005.07.066 (2005).
6. Gao, Q., Yuan, B. & Chess, A. Convergent projections of *drosophila* olfactory neurons to specific glomeruli in the antennal lobe. *Nature Neurosci.* **3**, 780–785, doi: 10.1038/77680 (2000).
7. Wang, F., Nemes, A., Mendelsohn, M. & Axel, R. Odorant receptors govern the formation of a precise topographic map. *Cell* **93**, 47–60, doi: 10.1016/S0092-8674(00)81145-9 (1998).
8. Mombaerts, P. *et al.* Visualizing an olfactory sensory map. *Cell* **87**, 675–686, doi: 10.1016/S0092-8674(00)81387-2 (1996).
9. Vassar, R. *et al.* Topographic organization of sensory projections to the olfactory bulb. *Cell* **79**, 981–991, doi: 10.1016/0092-8674(94)90029-9 (1994).
10. Malnic, B., Hirono, J., Sato, T. & Buck, L. B. Combinatorial Receptor Codes for Odors. *Cell* **96**, 713–723, doi: 10.1016/S0092-8674(00)80581-4 (1999).
11. Bushdid, C., Magnasco, M. O., Vosshall, L. B. & Keller, A. Humans can discriminate more than 1 trillion olfactory stimuli. *Science* **343**, 1370–1372, doi: 10.1126/science.1249168 (2014).
12. Turin, L. A spectroscopic mechanism for primary olfactory reception. *Chem. Senses* **21**, 773–791, doi: 10.1093/chemse/21.6.773 (1996).
13. Keller, A. & Vosshall, L. B. A psychophysical test of the vibration theory of olfaction. *Nat. Neurosci.* **7**, 337–338, doi: 10.1038/nn1215 (2004).
14. C. Araneda, R., Kini, A. D. & Firestein, S. The molecular receptive range of an odorant receptor. *Nature Neurosci.* **3**, doi: 10.1038/81774 (2000).
15. Brookes, J. C., Hartoutsiou, F., Horsfield, A. & Stoneham, A. Could Humans Recognize Odor by Phonon Assisted Tunneling? *Phys. Rev. Lett.* **98**, doi: 10.1103/PhysRevLett.98.038101 (2007).
16. Franco, M. I., Turin, L., Mershin, A. & Skoulakis, E. M. C. Molecular vibration-sensing component in *Drosophila melanogaster* olfaction. *Proc. Natl. Acad. Sci.* **108**, 3797–3802, doi: 10.1073/pnas.1012293108 (2011).
17. Pelz, D., Roeske, T., Syed, Z., Bruyne, M. D. & Galizia, C. G. The Molecular Receptive Range of an Olfactory Receptor *in vivo* (*Drosophila melanogaster* Or22a). *J. Neurobiol.* **66**, 1544–1563, doi: 10.1002/neu.20333 (2006).
18. Gabler, S., Soelster, J., Hussain, T., Sachse, S. & Schmucker, M. Physicochemical vs. Vibrational Descriptors for Prediction of Odor Receptor Responses. *Mol. Inform.* **32**, 855–865, doi: 10.1002/minf.201300037 (2013).
19. Schmucker, M., de Bruyne, M., Hähnel, M. & Schneider, G. Predicting olfactory receptor neuron responses from odorant structure. *Chem. Cent. J.* **1**, 11, doi: 10.1186/1752-153X-1-11 (2007).
20. Haddad, R., Carmel, L., Sobel, N. & Harel, D. Predicting the receptive range of olfactory receptors. *PLoS Comput. Biol.* **4**, doi: 10.1371/journal.pcbi.0040018 (2008).
21. Snitz, K. *et al.* Predicting odor perceptual similarity from odor structure. *PLoS Comput. Biol.* **9**, doi: 10.1371/journal.pcbi.1003184 (2013).
22. Yablonka, A., Sobel, N. & Haddad, R. & Biology, C. Odorant similarity in the mouse olfactory bulb. *Proc. Natl. Acad. Sci.* **109**, doi: 10.1073/pnas.1211623109 (2012).
23. Gane, S. *et al.* Molecular vibration-sensing component in human olfaction. *PLoS ONE* **8**, doi: 10.1371/journal.pone.0055780 (2013).
24. Turin, L., Gane, S., Georganakis, D., Maniati, K. & Skoulakis, E. M. Plausibility of the vibrational theory of olfaction. *Proc. Natl. Acad. Sci.* **112**, E3154–E3154, doi: 10.1073/pnas.1508035112 (2015).
25. Block, E. *et al.* Implausibility of the vibrational theory of olfaction. *Proc. Natl. Acad. Sci.* **112**, E2766–E2774, doi: 10.1073/pnas.1503054112 (2015).
26. Vosshall, L. B. Laying a controversial smell theory to rest. *Proc. Natl. Acad. Sci.* **112**, 6525–6526, doi: 10.1073/pnas.1507103112 (2015).
27. Buck, L. & Axel, R. A novel multigene family may encode odorant receptors: A molecular basis for odor recognition. *Cell* **65**, 175–187, doi: 10.1016/0092-8674(91)90418-X (1991).
28. Niimura, Y. Evolutionary dynamics of olfactory receptor genes in chordates: interaction between environments and genomic contents. *Hum. Genomics* **4**, 107, doi: 10.1186/1479-7364-4-2-107 (2009).

29. Sato, K. *et al.* Insect olfactory receptors are heteromeric ligand-gated ion channels. *Nature* **452**, 1002–1006, doi: 10.1038/nature06850 (2008).
30. Wicher, D. *et al.* Drosophila odorant receptors are both ligand-gated and cyclic-nucleotide-activated cation channels. *Nature* **452**, 1007–1011, doi: 10.1038/nature06861 (2008).
31. Nagel, K. I. & Wilson, R. I. Biophysical mechanisms underlying olfactory receptor neuron dynamics. *Nat. Neurosci.* **14**, 208–216, doi: 10.1038/nn.2725 (2011).
32. L. Jonesa, P., M. Paska, G., C. Rinkerb, D. & J. Zwiebel, L. Functional agonism of insect odorant receptor ion channels. *Proc. Natl. Acad. Sci.* **108**, 8821–8825, doi: 10.1073/pnas.1108410108 (2011).
33. Yao, C. A. & Carlson, J. R. Role of g-proteins in odor-sensing and CO₂-sensing neurons in drosophila. *The Journal of Neuroscience* **30**, 4562–4572, doi: 10.1523/JNEUROSCI.6357-09.2010 (2010).
34. Benton, R., Sachse, S., Michnick, S. W. & Vosshall, L. B. Atypical membrane topology and heteromeric function of Drosophila odorant receptors *in vivo*. *PLoS Biol.* **4**, doi: 10.1371/journal.pbio.0040020 (2006).
35. Smart, R. *et al.* Drosophila odorant receptors are novel seven transmembrane domain proteins that can signal independently of heterotrimeric G proteins. *Insect Biochem. Mol. Biol.* **38**, 770–780, doi: 10.1016/j.ibmb.2008.05.002 (2008).
36. C. Larsson, M. *et al.* Or83b encodes a broadly expressed odorant receptor essential for Drosophila olfaction. *Neuron* **43**, 703–714, doi: 10.1016/j.neuron.2004.08.019 (2004).
37. Wilson, R. I. Early Olfactory Processing in Drosophila: Mechanisms and Principles. *Annu. Rev. Neurosci.* 217–241, doi: 10.1146/annurev-neuro-062111-150533 (2014).
38. Kaupp, U. B. Olfactory signalling in vertebrates and insects: differences and commonalities. *Nat. Rev. Neurosci.* **11**, 188–200, doi: 10.1038/nrn2789 (2010).
39. Guerrieri, F., Schubert, M., Sandoz, J.-C. & Giurfa, M. Perceptual and neural olfactory similarity in honeybees. *PLoS Biol.* **3**, doi: 10.1371/journal.pbio.0030060 (2005).
40. Uchida, N., Takahashi, Y. K., Tanifuji, M. & Mori, K. Odor maps in the mammalian olfactory bulb: domain organization and odorant structural features. *Nature Neurosci.* **3**, 1035–1043, doi: 10.1038/79857 (2000).
41. Ramachandran, G., Ramakrishnan, C. & Sasisekharan, V. Stereochemistry of polypeptide chain configurations. *J. Mol. Biol.* **7**, 95–99 (1963).
42. Apostolakis, J., Plückthun, A. & Cafilisch, A. Docking small ligands in flexible binding sites. *J. Comput. Chem.* **19**, 21–37, doi: 10.1002/(SICI)1096-987X(19980115)19:1<21::AID-JCC2>3.0.CO;2-0 (1998).
43. Gunasekaran, K. & Nussinov, R. How different are structurally flexible and rigid binding sites? Sequence and structural features discriminating proteins that do and do not undergo conformational change upon ligand binding. *J. Mol. Biol.* **365**, 257–273, doi: 10.1016/j.jmb.2006.09.062 (2007).
44. Liang, J., Edelsbrunner, H. & Woodward, C. Anatomy of protein pockets and cavities: measurement of binding site geometry and implications for ligand design. *Protein Sci.* **7**, 1884, doi: 10.1002/pro.5560070905 (1998).
45. Zhang, Y. Progress and challenges in protein structure prediction. *Curr. Opin. Struct. Biol.* **18**, 342–348, doi: 10.1016/j.sbi.2008.02.004 (2008).
46. Lupieri, P., Nguyen, C. H. H., Bafghi, Z. G., Giorgetti, A. & Carloni, P. Computational molecular biology approaches to ligand-target interactions. *HFSP J.* **3**, 228–239, doi: 10.2976/1.3092784 (2009).
47. Khafizov, K., Anselmi, C., Menini, A. & Carloni, P. Ligand specificity of odorant receptors. *J. Mol. Model* **13**, 401–409, doi: 10.1007/s00894-006-0160-9 (2007).
48. Man, O., Gilad, Y. & Lancet, D. Prediction of the odorant binding site of olfactory receptor proteins by human-mouse comparisons. *Protein Sci.* **13**, 240–254, doi: 10.1110/ps.03296404 (2004).
49. C. Lai, P., Singer, M. S. & Crasto, C. J. Structural activation pathways from dynamic olfactory receptor-odorant interactions. *Chem. Senses* **30**, 781–792, doi: 10.1093/chemse/bji070 (2005).
50. Vaidehi, N. *et al.* Prediction of structure and function of g protein-coupled receptors. *Proc. Natl. Acad. Sci.* **99**, 12622–12627, doi: 10.1073/pnas.122357199 (2002).
51. Floriano, W. B., Vaidehi, N. & Goddard, W. a. Making sense of olfaction through predictions of the 3-D structure and function of olfactory receptors. *Chem. Senses* **29**, 269–290, doi: 10.1093/chemse/bjh030 (2004).
52. Schmiedeberg, K. *et al.* Structural determinants of odorant recognition by the human olfactory receptors OR1A1 and OR1A2. *J. Struct. Biol.* **159**, 400–412, doi: 10.1016/j.jsb.2007.04.013 (2007).
53. Katada, S., Hirokawa, T., Oka, Y., Suwa, M. & Touhara, K. Structural basis for a broad but selective ligand spectrum of a mouse olfactory receptor: mapping the odorant-binding site. *J. Neurosci.* **25**, 1806–15, doi: 10.1523/JNEUROSCI.4723-04.2005 (2005).
54. Kato, A., Katada, S. & Touhara, K. Amino acids involved in conformational dynamics and G protein coupling of an odorant receptor: targeting gain-of-function mutation. *J. Neurochem.* **107**, 1261–1270, doi: 10.1111/j.1471-4159.2008.05693.x (2008).
55. Rospars, J.-P. Interactions of odorants with olfactory receptors and other preprocessing mechanisms: how complex and difficult to predict? *Chem. Senses* **38**, 283–287, doi: 10.1093/chemse/bjt004 (2013).
56. Galizia, C. G., Münch, D., Strauch, M., Nissler, A. & Ma, S. Integrating heterogeneous odor response data into a common response model: A DoOR to the complete olfactome. *Chem. Senses* **35**, 551–563, doi: 10.1093/chemse/bjq042 (2010).
57. De Bruyne, M., J. Clyne, P. & R. Carlson, J. Odor coding in a model olfactory organ: The drosophila maxillary palp. *J. Neurosci.* **19**, 4520–4532 (1999).
58. De Bruyne, M., Foster, K. & R. Carlson, J. Odor coding in the drosophila antenna. *Neuron* **30**, 537–552, doi: 10.1016/S0896-6273(01)00289-6 (2001).
59. A. Dobritsa, A., van Naters, W. v. d. G., G. Warr, C., Steinbrecht, R. & R. Carlson, J. Integrating the molecular and cellular basis of odor coding in the drosophila antenna. *Neuron* **37**, 827–841, doi: 10.1016/S0896-6273(03)00094-1 (2003).
60. Goldman, A. L., Van der Goes van Naters, W., Lessing, D., Warr, C. G. & Carlson, J. R. Coexpression of two functional odor receptors in one neuron. *Neuron* **45**, 661–666, doi: 10.1016/j.neuron.2005.01.025 (2005).
61. Hallem, E. A., Ho, M. G. & Carlson, J. R. The molecular basis of odor coding in the drosophila antenna. *Cell* **117**, 965–979, doi: 10.1016/j.cell.2004.05.012 (2004).
62. Hallem, E. A. & Carlson, J. R. Coding of odors by a receptor repertoire. *Cell* **125**, 143–160, doi: 10.1016/j.cell.2006.01.050 (2006).
63. Kreher, S. A., Kwon, J. Y. & Carlson, J. R. The molecular basis of odor coding in the Drosophila larva. *Neuron* **46**, 445–456, doi: 10.1016/j.neuron.2005.04.007 (2005).
64. Kreher, S. A., Mathew, D., Kim, J. & Carlson, J. R. Translation of sensory input into behavioral output via an olfactory system. *Neuron* **59**, 110–124, doi: 10.1016/j.neuron.2008.06.010 (2008).
65. Kwon, J. Y., Dahanukar, A., Weiss, L. A. & Carlson, J. R. The molecular basis of CO₂ reception in Drosophila. *Proc. Natl. Acad. Sci.* **104**, 3574–3578, doi: 10.1073/pnas.0700079104 (2007).
66. Stensmyr, M. C., Giordano, E., Balloi, A., Angioy, A.-M. & S. Hansson, B. Novel natural ligands for Drosophila olfactory receptor neurones. *J. Exp. Biol.* **206**, 715–724, doi: 10.1242/jeb.00143 (2003).
67. Turner, S. L. & Ray, A. Modification of CO₂ avoidance behaviour in Drosophila by inhibitory odorants. *Nature* **461**, 277–281, doi: 10.1038/nature08295 (2009).
68. van Naters, W. v. d. G. & Carlson, J. R. Receptors and neurons for fly odors in drosophila. *Curr. Biol.* **17**, 606–612, doi: 10.1016/j.cub.2007.02.043 (2007).

69. Yao, C. A., Ignell, R. & Carlson, J. R. Chemosensory coding by neurons in the coeloconic sensilla of the *Drosophila* antenna. *J. Neurosci.* **25**, 8359–8367, doi: 10.1523/JNEUROSCI.2432-05.2005 (2005).
70. Münch, D. & Galizia, C. G. Door 2.0 - comprehensive mapping of drosophila melanogaster odorant responses. *Sci. Rep.* **6**, 21841, doi: 10.1038/srep21841 (2016).
71. De Bruyne, M., Smart, R., Zammit, E. & Warr, C. G. Functional and molecular evolution of olfactory neurons and receptors for aliphatic esters across the drosophila genus. *J. Comp. Physiol. A* **196**, 97–109, doi: 10.1007/s00359-009-0496-6 (2010).
72. Dweck, H. K., Ebrahim, S. A., Farhan, A., Hansson, B. S. & Stensmyr, M. C. Olfactory proxy detection of dietary antioxidants in drosophila. *Curr. Biol.* **25**, 455–466, doi: 10.1016/j.cub.2014.11.062 (2015).
73. Dweck, H. K. *et al.* Olfactory preference for egg laying on citrus substrates in drosophila. *Curr. Biol.* **23**, 2472–2480, doi: 10.1016/j.cub.2013.10.047 (2013).
74. Marshall, B., Warr, C. G. & De Bruyne, M. Detection of volatile indicators of illicit substances by the olfactory receptors of drosophila melanogaster. *Chem. Senses* **35**, 613–625, doi: 10.1093/chemse/bjq050 (2010).
75. Montague, S. A., Mathew, D. & Carlson, J. R. Similar odorants elicit different behavioral and physiological responses, some supersustained. *J. Neurosci.* **31**, 7891–7899, doi: 10.1523/JNEUROSCI.6254-10.2011 (2011).
76. Pedretti, A., Villa, L. & Vistoli, G. VEGA - An open platform to develop chemo-bio-informatics applications, using plug-in architecture and script programming. *J. Comput.-Aided Mol. Des.* **18**, 167–173, doi: 10.1023/B:JCAM.0000035186.90683.f2 (2004).
77. R Core Team. *R: A Language and Environment for Statistical Computing*. R Foundation for Statistical Computing, Vienna, Austria (2014). URL <http://www.R-project.org/>.
78. Benjamini, Y. & Hochberg, Y. Controlling the false discovery rate: a practical and powerful approach to multiple testing. *J. R. Statist. Soc. B* **57**, 289–300 (1995).
79. Shaffer, J. P. Multiple hypothesis testing. *Annu. Rev. Psychol.* **46**, 561–584, doi: 10.1146/annurev.ps.46.020195.003021 (1995).
80. Moody, S. L., Wise, S. P., di Pellegrino, G. & Zipser, D. A model that accounts for activity in primate frontal cortex during a delayed matching-to-sample task. *J. Neurosci.* **18**, 399–410 (1998).
81. Freedman, D. J., Riesenhuber, M., Poggio, T. & Miller, E. K. Experience-dependent sharpening of visual shape selectivity in inferior temporal cortex. *Cereb. Cortex* **16**, 1631–1644, doi: 10.1093/cercor/bhj100 (2006).
82. Zarzo, M. Hedonic judgments of chemical compounds are correlated with molecular size. *Sensors* **11**, 3667–3686, doi: 10.3390/s110403667 (2011).
83. Xu, P. X., Atkinson, R., Jones, D. N. & Smith, D. P. *Drosophila* obp lush is required for activity of pheromone-sensitive neurons. *Neuron* **45**, 193–200, doi: 10.1016/j.neuron.2004.12.031 (2005).
84. Gomez-Diaz, C., Reina, J. H., Cambillau, C. & Benton, R. Ligands for pheromone-sensing neurons are not conformationally activated odorant binding proteins. *PLoS Biol.* doi: 10.1371/journal.pbio.1001546 (2013).
85. Mainland, J. D., Li, Y. R., Zhou, T., Liu, W. L. & Matsunami, H. Human olfactory receptor responses to odorants. *Sci. Data* **2**, doi: 10.1038/sdata.2015.2 (2015).
86. Tirandaz, A., Ghahramani, F. T. & Shafiee, A. Dissipative vibrational model for chiral recognition in olfaction. *Phys. Rev. E* **92**, 032724, doi: 10.1103/PhysRevE.92.032724 (2015).

Acknowledgements

We are especially grateful to B. N. Araabi, S. Aghvami, N. Doostani and Shima Seyed-Allaei for the careful reading of the manuscript.

Author Contributions

M.S. and H.S.-a. equally contributed to the design of the study. H.S.-a. developed the mathematical framework. M.S. prepared and analyzed the data. H.S.-a. created Figure 1, and M.S. produced all other figures. H.S.-a. wrote the article, and M.S. generated the bibliography. Both authors have reviewed the manuscript.

Additional Information

Supplementary information accompanies this paper at <http://www.nature.com/srep>

Competing financial interests: The authors declare no competing financial interests.

How to cite this article: Saberi, M. and Seyed-allaei, H. Odorant receptors of *Drosophila* are sensitive to the molecular volume of odorants. *Sci. Rep.* **6**, 25103; doi: 10.1038/srep25103 (2016).



This work is licensed under a Creative Commons Attribution 4.0 International License. The images or other third party material in this article are included in the article's Creative Commons license, unless indicated otherwise in the credit line; if the material is not included under the Creative Commons license, users will need to obtain permission from the license holder to reproduce the material. To view a copy of this license, visit <http://creativecommons.org/licenses/by/4.0/>